Confronting Models with Atmospheric Radiation Measurement Data: A Statistical Comparison of Southern Great Plains Atmospheric Emitted Radiance Interferometer Radiance Spectra and Global Climate Models Output

J.A. Dykema, S.S. Leroy, B.F. Farrell, and J.G. Anderson
Harvard University
Division of Engineering and Applied Science
Cambridge, Massachusetts

D. Tobin, R. Knuteson, and H. Revercomb
University of Wisconsin – Madison
Space Science and Engineering Center
Madison, Wisconsin

X. Huang
National Oceanic and Atmospheric Administration – Geophysical Fluid Dynamics Laboratory
Princeton University Forrestal Campus
Princeton, New Jersey

Introduction

Forecasts of decadal climate change at subcontinental scales made by global climate models (GCMs) are currently too uncertain to be useful to policy makers. For example, the forecasts of global mean surface temperatures in the current Intergovernmental Panel on Climate Change (IPCC) Special Report on Emissions (SRES) A1B scenario show an agreement across 15 models of about ±0.75 K in warming of the global mean temperature after 100 yearr. At the subcontinental scale, the disagreement in surface temperatures at high latitudes can range as large 15 K in extreme cases for the 100-year forecast. Forecasts of precipitation and extreme weather show even more variation for these IPCC emission scenarios.

The disagreement between low cloud representations in models manifests itself in Atmospheric Radiation Measurement (ARM) data in a unique way. Measurements from the ARM atmospheric emitted radiance interferometer (AERI) instrument at the Southern Great Plains (SGP) site strongly constrain low cloud behavior. For example, they indicate that NWP models predict liquid water paths for low clouds that are three times the observed value (Sengupta et al. 2004). Measurements of top of the atmosphere radiance have revealed that inadequate cloud representation in climate models causes the radiative balance to lack realistic long-term variability (Cess et al. 2001; Wielicki et al. 2002). Upward looking radiance measured from the surface, as by AERI, is sensitive to a different portion of the

atmospheric state than satellite measurements, providing detailed information from the surface up to about 3 km. The AERI radiances are therefore well-suited to investigating the failure of models to produce realistic distribution of low-level clouds.

The key requirement for developing an accurate climate forecast is that the forecast model must contain the correct relationship between anticipated forcings and the response in climatological variables of interest. This relationship is not captured by the mean statistics of the climate system, but rather by the second moment statistics, as defined by the covariances of observable properties of the climate system. This concept derives from a formulation of the fluctuation-dissipation theorem applied to the climate by Leith (1975). We seek a methodology that extracts the required covariances from climate observations in a form which allows for the testing and improvement of climate models. This method is provided by Linear Inverse Modeling (LIM), a technique which extracts the dynamical relationship between climate variables directly from observations (Penland and Magorian 1993). The power of LIM derives from its ability to obtain dynamics from any well-observed, representative measurement of the climate system. It has been demonstrated in other climate applications using a variety of datasets, and it can also be applied directly to improving low level cloud parameterizations using ARM radiation measurements, entirely without the use of a retrieval algorithm. In this work, we choose to probe the dynamics of the AERI radiances. These radiances contain detailed information about the distribution of temperature, water vapor and clouds in the boundary layer. The correctly determined dynamical relationship among these variables provides a powerful constraint on the representation of the boundary layer in a climate model. This constraint must be satisfied for any model to forecast future climate credibly.

The Atmospheric Emitted Radiance Interferometer

The AERI acquires calibrated spectra of downwelling infrared radiation at a nominal spectral resolution of 1 wavenumber (~0.48 cm^{-1} unapodized) from 520 cm^{-1} to 3020 cm^{-1} (3.3 to 19.2 μm), yielding 5000 channels per measurement. The spectral calibration (wavelength scale) is known to better than 0.3 ppm (3-sigma). The standard zenith sky view is integrated over 3.5 min. within a field of view (FOV) of 15 mrad half angle. A full description of the design and radiometric calibration of the instrument is available in Knuteson et al. (2004). A 10-year dataset of AERI measurements recorded at the surface is contained in the Department of Energy ARM Data Archive. The measurements were recorded at 8-10 minute intervals during this period.

The AERI radiances provide high vertical resolution profiles of water vapor and temperature to 3 km (Feltz et al. 2003). In regions of strong atmospheric absorption around 700 cm^{-1} and from 1400-1600 cm^{-1} the spectrum is dominated by temperature a few meters from the instrument. Water vapor lines reveal the structure of the water vapor profile between 1100-1400 cm^{-1} and below 600 cm^{-1}. The atmospheric window region (800-1000 cm^{-1}) is dominated by sensitivity to clouds. Outside of the opaque spectral regions, variability is dominated by the presence or absence of clouds. The high spectral resolution provides sensitivity to cloud microphysics.

All of the above features make AERI data an attractive dataset for testing climate models. The high temporal resolution captures the interplay of water vapor, temperature, clouds and winds in the lowermost 3 km of the atmosphere. This interplay in turn modulates the surface energy budget, which is an important component of the cloud-radiation feedback and the overall climate.

Producing Atmospheric Emitted Radiance Interferometer-like Radiances from Global Climate Models

Traditional evaluations of climate models with spectrally resolved radiance measurements have been performed through retrievals of the canonical meteorological variables. An advantage of the methods developed in this study is that they work directly on the calibrated radiance observations. It is a straightforward matter to calculate model radiances that can be directly compared to the AERI measurements. The climate models are run, archiving profiles of temperature, humidity, and clouds, at a temporal resolution of eight times per day or higher. Combined with trace gas profiles, the data provide a time series of inputs to the moderate-resolution atmospheric radiance and transmittance model radiation code, which produces a time series of resolved infrared radiance spectra. The spectra are calculated over the spectral interval from 1 cm^{-1} to 3300 cm^{-1}, fully overlapping the both channels of the AERI measurements. These examples are confined to AERI channel 1, covering from approximately 520 cm^{-1} to 1700 cm^{-1}, and accounting for over 80% of the infrared radiance emitted by the atmosphere. For the investigation of the Geophysical Fluid Dynamics Laboratory (GFDL) model shown here, the AM2 model (GFDL's Global Atmosphere Model Development Team 2003) was forced with the Hurrell sea surface temperatures (SSTs) for the period from September 2000-September 2002. Profiles of ozone and aerosols are derived from the Mozart chemical transport model.

Linear Stochastic Modeling: An Approach to Model Assessment and Comparison

Second moments of meteorological variables of the climate system are strongly related to the sensitivity of that system to external forcing. This is an application of fluctuation-dissipation theory as formalized by Leith (1975). Accordingly, the sensitivity of a climate variable u_α to set of constant, infinitesimal forcings $\delta\dot{u}_\beta$ is given by:

$$\delta\dot{u}_\alpha(t) = \int_{-\infty}^{t} g_{\alpha\beta}(t-t')\,\delta\dot{u}_\beta(t')\,dt' \qquad (1)$$

where $g_{\alpha\beta}(\tau)$, the α,β element of matrix g(τ), in the limit of Gaussian statistics, is specified by:

$$\mathbf{g}(\tau) = \mathbf{U}(\tau)\,\mathbf{U}^{-1}(0) \qquad (2)$$

Here $\mathbf{U}(\tau)$ represents the lagged covariance matrix of the variables u_α at lag time τ. Hence the sensitivity of the u_α to forcing by u_β is proportional to the covariance of u_α and u_β. The sensitivity of the climate may therefore be measured directly by appropriate observations of the short-term fluctuations of the climate that constitute natural variability. Cionni et al. (2004) show that the value of the sensitivity of a GCM to external forcing is predicted correctly by fluctuation-dissipation theory.

Empirical Orthogonal Functions: A Basis Set for Atmospheric Emitted Radiances Interferometer Radiances

A convenient technique for representing the information contained in the second moment statistics is that of empirical orthogonal function (EOF) analysis. We have applied this type of analysis to spectrally resolved infrared radiances (Haskins et al. 1997; Haskins et al. 1999; Huang et al. 2002), uncovering essential features of atmospheric behavior. In Figure 1 we show the first four principal components (PCs) of variability in AERI spectra as seen in the time series of measurements from the SGP site for the period 1998-2003, and in AERI-like radiances calculated for GFDL for September 2000 – September 2002. Principal components are EOFs scaled by the square root of their associated eigenvalues. The first principal component is the signature of a cloud and accounts for 77.4% of total variance in the infrared. The second principal component shows a pattern of anticorrelation between the warming near the surface and cooling aloft and accounts for 20.8% of the total variance in the infrared. The model PCs compare favorably with the measurement PCs in light of the large difference between PCs derived from satellites and models (Huang et al. 2002). Taken together, the first two PCs contribute two pieces of information on low clouds: whether or not a cloud is present, and what the height and thickness of the cloud is. The third and fourth PCs are related to the fluctuations in the atmospheric column due to the diurnal and semidiurnal cycle.

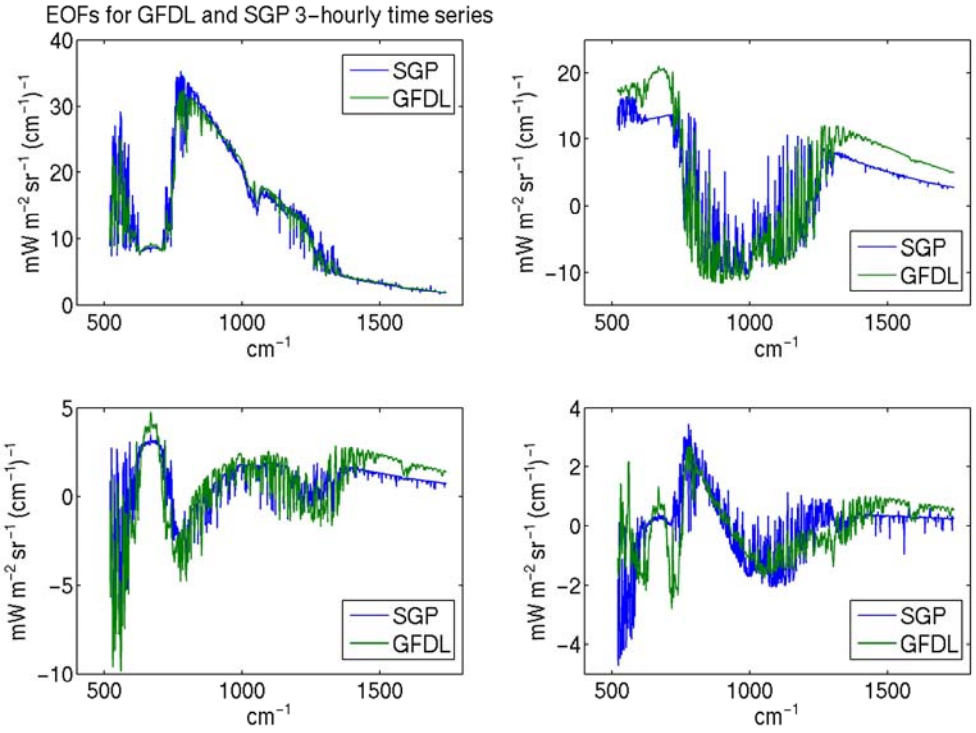

Figure 1. Principal components (PCs) calculated for time series of AERI SGP and simulated GFDL. The AERI spectra are three hour averages, the model spectra are calculated from eight times daily model output. The excessive variability of the model radiances in captured in the second PC. These PCs account for 77.4%, 20.8%, 1.0%, and 0.4% of the total variance, respectively.

The timescales associated with the variability captured by these principal components may be inferred by projecting the EOFs onto the time series of radiances, and analyzing the resulting time series of coefficients. Inspection of the time series for these coefficients for EOF1 and EOF2 clearly reveals a substantial contribution of annual variability to the first two EOFs, as shown in the upper panel of Figure 2. This annual variability causes the existence of clusters in the probability distribution function of these EOFs, which will be shown below to complicate the process of uncovering the system dynamics. The contribution of these periodic fluctuations may be calculated using singular spectral analysis (Vautard and Ghil 1989). Singular spectral analysis is a technique that determines an optimal basis set for a time series, capturing the variability in fewer basis functions than fourier analysis. Applying singular spectral analysis (SSA) to the time series of EOF1 and EOF2 coefficents reveals that the first two singular spectra, possessing a period of approximately one year, accounts for 27.0% of the variability for EOF1 and 48.3% for EOF2. By projecting these singular spectra onto the time series, a similar set of coefficients is created which provides an optimal reconstruction of the original time series. Applying this procedure for the first two singular spectra allows an approximate removal of the annual cycle from the time series of EOF1 and EOF2 coefficients, as shown in the lower panel of Figure 2.

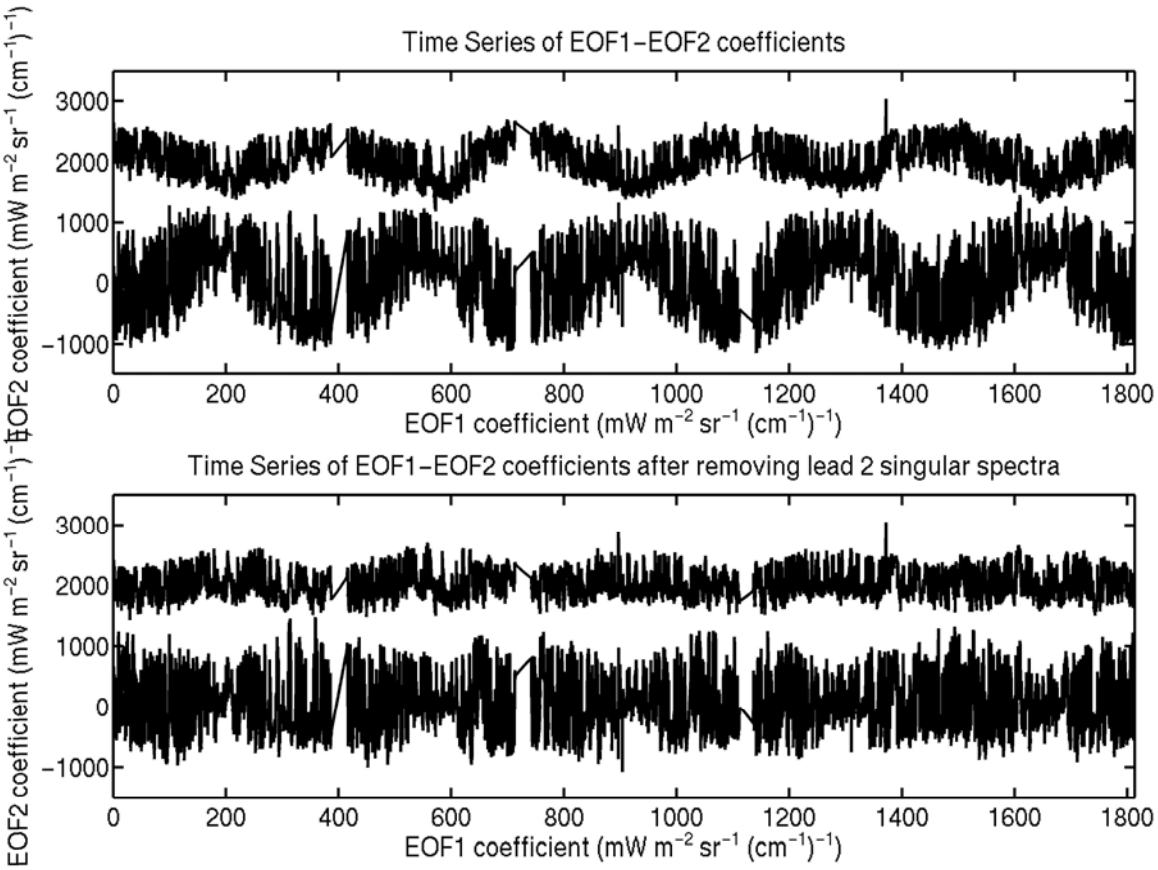

Figure 2. The time series of coefficients for EOF1 and EOF2 from the AERI SGP in the top panel show the contribution of the seasonal cycle to the dynamics of the radiance spectrum. The time series for EOF2 is displaced above the EOF1 time series for clarity. The seasonal cycle may be reduced by subtracting the leading two singular spectra (found via SSA, see text) from the time series, as shown in the lower panel.

A Review of Linear Stochastic Modeling

Although ultimately governed by a highly nonlinear system, the dynamics of perturbations to the climate state ϕ about the equilibrium point of the statistically stationary climate are approximately governed by the linear stochastic equation:

$$\frac{d\phi}{dt} = \mathbf{A}\phi + \mathbf{F}\varepsilon(t) \tag{3}$$

where *A* is a linear operator and $\mathbf{F}\varepsilon(t)$ is a stochastic forcing accounting for the fast nonlinear processes (Farrell and Ioannou 1996). Climate statistics are predicted with surprising accuracy by this linear stochastic modeling (Farrell and Ioannou 1995; Zhang and Held 1999; Whitaker and Sardeshmukh 1998), admitting powerful linear analysis methods. The accurate approximation to statistical dynamics provided by such linear stochastic systems motivates the attempt to obtain approximations to the above equation from AERI observations for the purpose of comparison with model behavior.

Zero time-lag statistics as revealed by the EOFs above are insufficient to evaluate the dynamic processes underlying the distribution of boundary layer clouds. LIM is well-suited to determining the character of this process from observations, extracting the system dynamics **A** directly from the lagged covariances **U** calculated from observations such as AERI. How the climatology of complex and turbulent atmospheric flows is amenable to such a reduction was examined by DelSole and Farrell (1996) who were able to extract from nonlinear simulations of a two-layer baroclinic channel flow the effective linear operator that was controlling the climatology of the channel flow. DelSole and Hou (1999) extended these methods to demonstrate the accuracy of LIM in inverting the GCM time series for the climatology of a full hemispheric GCM. Additionally, successful modeling of the intraseasonal variability of the midlatitude atmosphere in the traditional variables of velocity and temperature, and of El Nino-Southern Oscillation dynamics in the SST have been achieved with these methods (Farrell and Ioannou 1995; Penland and Magorian 1993). Of particular interest to us is that the LIM method is not confined to traditional variables such as velocity and temperature; it can be applied to obtain intrinsic dynamics of a system in any variable. The advantage of this approach is that it provides information on the primary structures of the system response and their temporal variability together with a link among the structures in the form of a dynamical system. We believe that analysis of the intrinsic dynamics of the radiance spectrum captures much more information on the spectra and their temporal variability than an analysis of quantities retrieved from the radiation spectrum. Comparison among models and between models and data can be sensitively made by contrasting their structure and dynamics using this method.

LIM provides a convenient framework for comparing model and observed dynamics, obtaining the matrix of the intrinsic dynamics, **A**, and an equivalent stochastic forcing matrix, **F**, in the dynamical system described by equation 3. The dynamics are identified from observations of the covariance and lag covariance of ϕ denoted by $\mathbf{C}(0)$ and $\mathbf{C}(\tau)$, respectively, as follows:

$$\mathbf{A} = \ln\left(\frac{\mathbf{C}(\tau)\mathbf{C}^{-1}(0)}{\tau}\right)$$
$$\mathbf{F}\mathbf{F}^{\dagger} = (-\mathbf{A}\mathbf{C} + \mathbf{C}\mathbf{A}^{\dagger}) \qquad (4)$$

Here ϕ refers to resolved radiances from AERI observations and calculated from a historical SST run of the GFDL AM2 model. We wish to uncover the intrinsic dynamics of the AERI radiances, expressed as a time series of EOFs. By projecting the time series of AERI radiances on to the leading EOFs, we represent a very large fraction of the variability in the radiances in a space of drastically reduced dimension. For this study, only the first four EOFs are kept. The dynamics are then obtained by calculating the matrix **A** from the covariances of this four dimensional time series according to equation 2. For ease of visualization, the dynamics are obtained for two EOFs at a time, resulting in a 2 x 2 matrix.

Despite the good agreement between the model and measured EOF3 and EOF4 shown in Figure 1, the model dynamics are substantially different from the intrinsic dynamics of the measurement, as shown in Figure 3. The dynamics obtained from LIM are represented as a vector field in Figure 3 and Figure 4. The streamlines in this vector field show the mean temporal evolution of the radiances projected into the space of the EOFs. This trajectory of the atmosphere in time is illustrated in Figure 4 by the points superimposed on the vector field, which correspond to three AERI observations each separated by three hours. The plot of the three radiance spectra in Figure 4 shows how the deviation of these AERI spectra from the mean value, projected into the space of EOF3 and EOF4, develops over the course of six hours. Although it is convenient to visualize this dynamics in two dimensions, LIM can obtain a higher-dimensional dynamics, capturing the coupled evolution in time of the dominant degrees of freedom in the atmosphere. A powerful characteristic of LIM is that it can uncover correlated structures among EOFs, which are forced to be uncorrelated at zero time lag.

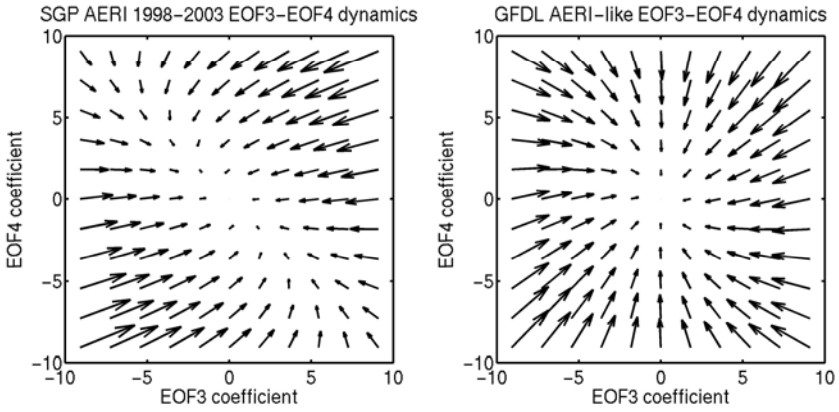

Figure 3. Despite the similarity of the model simulation and observed radiances revealed by the comparisons of the third and fourth PCs in Figure 1, substantial differences exist in the underlying dynamics of the atmosphere, as shown by the dynamics obtained with LIM. The left hand panel, which represents the linearized operator **A** for EOF3 and EOF4 in the SGP radiances, reveals a diffusive dynamics. The dynamics of the GFDL model as represented by the vector field in the right hand panel show that excitations of EOF3 and EOF4 show simple contraction back to equilibrium.

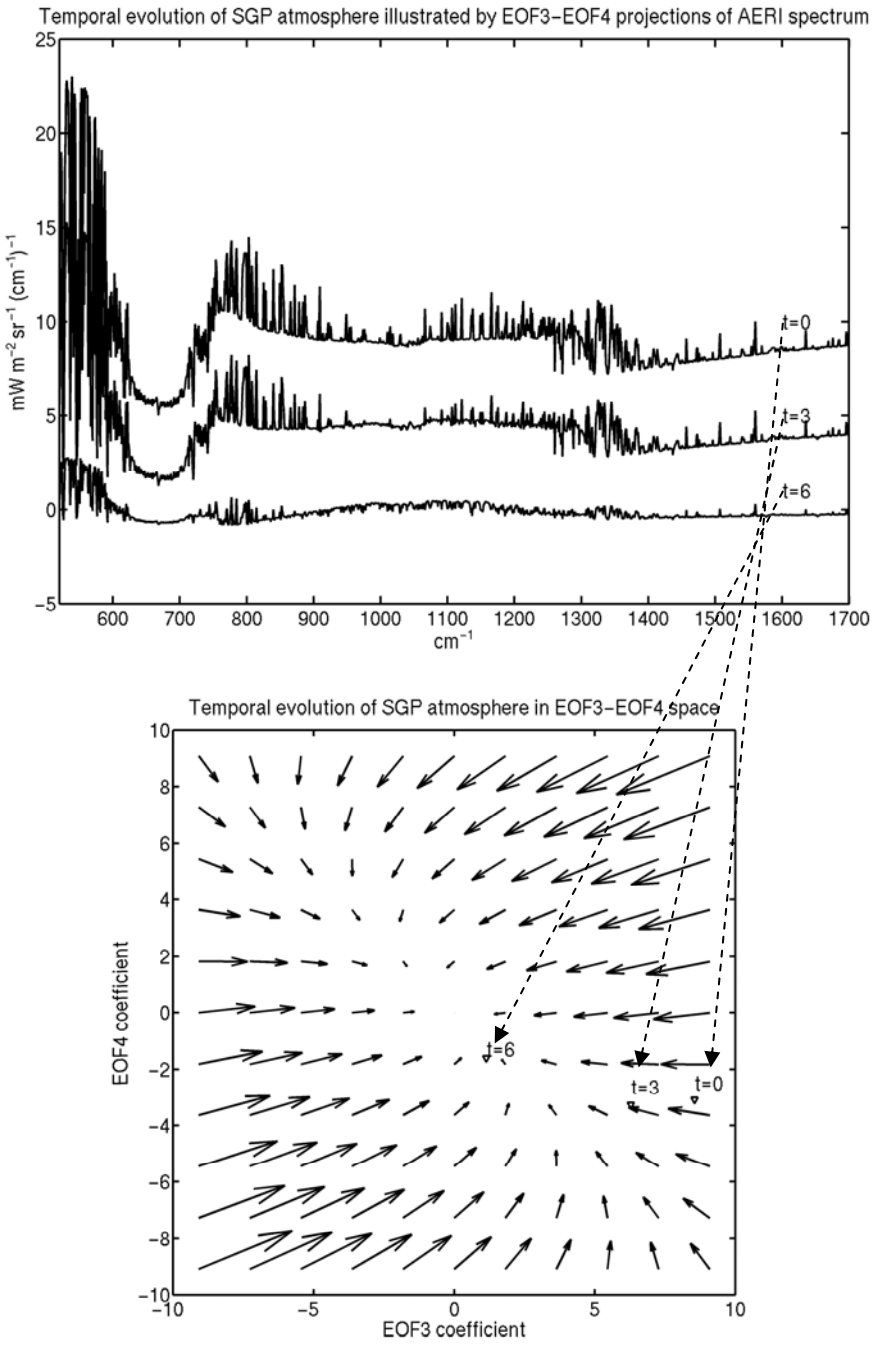

Figure 4. The dynamics of the EOF3 and EOF4 in the AERI radiance time series may be visualized as a vector field, as shown in the lower panel. The evolution of the radiance over a six-our period is indicated by the triangles superimposed on the vector field, and labeled “t=0”, “t=3”, and “t=6.” The top panel indicates the sum of the EOF3 and EOF4 components of the radiance at these time steps, matched to the corresponding points in the vector field by the dotted lines. As can be seen from this figure, the system will tend to evolve along the streamlines of the vector field defined by the equivalent linear operator **A**.

LIM reveals additional information is contained in the temporal dynamics of the AERI radiances. The same physical influence seems produce the radiance EOFs in both the AERI measurements and the model simulations, judging by the similarity in their PCs. The differences between the model and observations are only uncovered by obtaining and comparing the dynamical model controlling them. Because of the sensitivity of the AERI radiances to the vertical structure of temperature and water vapor up to 3 km, along with the height and thickness of clouds and the presence of aerosols, this dynamical system captures the subgrid scale physical processes controlling the model distribution of low-level clouds and precipitation. The comparison of the LIM and the underlying dynamics of this complex turbulent system can be used to identify and improve boundary layer parameterizations (Del Sole and Farrell 1998).

Conclusions

We have analyzed the second moment statistics of downwelling infrared radiation spectra measured by the ARM AERI instrument at the SGP site. We have applied EOF analysis to extract the dominant structures of atmospheric variability, and reduce the dimensionality of the time series of radiance data. Using the EOF to produce a reduced representation of the AERI data, we have applied LIM to obtain the intrinsic dynamics. These dynamics capture the coupling of temperature, water vapor and clouds in the lower atmosphere.

Because of the relationship between cloud processes and the radiation budget, correctly reproducing this dynamical behavior is essential to accurate decadal-to-centennial scales forecasts of future climate. By bringing the dynamics of temperature, water vapor and clouds of the model into agreement with the dynamics revealed from the observations by LIM, the model representation of clouds and associated radiative processes will be improved. These techniques provide a rigorous test for climate model performance that exploit the dense information content of the radiance measurements themselves, and suggest a path towards model improvement.

References

Cess, RD, M Zhang, BA Wielicki, DF Young, X-L Zhou, and Y Nikitenko. 2001. "The influence of the 1998 El Niño upon cloud-radiative forcing over the Pacific warm pool." *Journal of Climate* 14, 2129-2137.

Cionni, I, G Visconti, and F Sassi. 2004. "Fluctuation dissipation theorem in a general circulation model." *Geophysical Research Letters* 31(9), L09206.

DelSole, T, and BF Farrell. 1996. "The quasi-linear equilibration of a thermally maintained, stochastically excited jet in a quasigeostrophic model." *Journal of Atmospheric Sciences* 53(13), 1781-1797.

DelSole, T, and AY Hou. 1999. "Empirical stochastic models for the dominant climate statistics of a general circulation model." *Journal of Atmospheric Science* 56, 3436.

Farrell, BF, and PJ Ioannou. 1995. "Stochastic dynamics of the midlatitude atmospheric jet." *Journal of Atmospheric Science* 52(10), 1642–1656.

Farrell, BF, and PJ Ioannou. 1996. "Generalized stability theory .1. Autonomous operators." *Journal of Atmospheric Science* 53(14), 2025–2040.

Feltz, WF, HB Howell, RO Knuteson, HM Woolf, and HE Revercomb. 2003. "Near Continuous Profiling of Temperature, Moisture, and Atmospheric Stability using the Atmospheric Emitted Radiance Interferometer (AERI)." *Journal of Applied Meteorology* 42, 584-597.

GFDL's GAMDT (Global Atmosphere Model Development Team). 2004. "The new GFDL global atmosphere and land model AM2/LM2: Evaluation with prescribed SST simulations." Revised for *Journal of Climate*.

Haskins, R, R Goody, and L Chen. 1997. "Radiance covariance and climate models." *Journal of Climate* 12(5), 1409–1422.

Haskins, RD, RM Goody, and L Chen. 1999. "A statistical method for testing a general circulation model with spectrally resolved satellite data." *Journal of Geophysical Research* 102(D14), 16563-16581.

Huang, X, J Farrara, SS Leroy, YL Yung, and RM Goody. 2002. "Cloud variability as revealed in outgoing infrared spectra: comparing model to observation with spectral EOF analysis." *Geophysical Research Letters* 29(8), 111–114.

IPCC. 2001. Climate Chance 2001: The Scientific Basis, Contribution of Working Group I to the Third Assessment Report of the Intergovernmental Panel on Climate Change. New York: Cambridge University Press.

Knuteson RO, HE Revercomb, FA Best, NC Ciganovich, RG Dedecker, TP Dirkx, SC Ellington, WF Feltz, RK Garcia, HB Howell, WL Smith, JF Short, and DC Tobin. 2004. "Atmospheric Emitted Radiance Interferometer (AERI) Part I: Instrument Design." *Journal of Atmospheric Oceanic Technology* 21, 1763–1776.

Leith, CE. 1975. "Climate response and fluctuation dissipation." *Journal of Atmospheric Science* 32(10), 2022–2026.

Penland, C, and T Magorian. 1993. "Prediction of Niño 3 sea surface temperatures using linear inverse modeling." *Journal of Climate* 6(6), 1067–1076.

Sengupta, M, EE Clothiaux, and TP Ackerman. 2004. "Climatology of warm boundary layer clouds at the ARM SGP site and their comparison to models." *Journal of Climate* 17(24), 4760-4782.

Vautard, R, and M Ghil. 1989. "Singular spectrum analysis in nonlinear dynamics with applications to paleoclimatic time series." *Physica D* 35, 395-424.

Whitaker, JS, and PD Sardeshmukh. 1998. "A linear theory of extratropical synoptic eddy statistics." *Journal of Atmospheric Science* 55, 237–258.

Wielicki, BA, TM Wong, RP Allan, A Slingo, JT Kiehl, BJ Soden, CT Gordon, AJ Miller, SK Yang, DA Randall, F Robertson, J Susskind, and H Jacobowitz. 2002. "Evidence for large decadal variability in the tropical mean radiative energy budget." *Science* 295 (5556): 841-844.

Zhang, Y, and IM Held. 1999. "A linear stochastic model of a GCM's midlatitude storm tracks." *Journal of Atmospheric Science* 56(19), 3416–3435.